Yang *et al. Cell Communication and Signaling* (2025) 23:222
https://doi.org/10.1186/s12964-025-02221-z

Cell Communication and Signaling

RESEARCH Open Access

RYBP promotes HIV-1 latency through promoting H2AK119ub and decreasing H3K4me3

Xinyi Yang[1,2*†], Yuqi Zhu[1†], Xiaying Zhao[1†], Jingna Xun[1,3], Xingyu Wang[1], Yipeng Cheng[1], Su Xiong[1], Xingwen Yu[1], Suixiang Li[1], Danqing Wang[2], Zhiliang Hu[4], Yinzhong Shen[3,5], Shibo Jiang[7], Hongzhou Lu[6], Gang Wang[1] and Huanzhang Zhu[1*]

Abstract

Background Acquired immunodeficiency syndrome (AIDS) cannot be completely cured, and the main obstacle is the existence of viral reservoirs. However, we currently do not fully understand the molecular mechanisms by which HIV-1 latency is established and maintained.

Methods Here, based on engineered chromatin immunoprecipitation (enChIP) technology that using FLAG-tagged zinc finger nucleic acid proteins (FLAG-ZFP) that bind to the HIV-1 L region and chromatin immunoprecipitation, we identified RYBP as a new HIV-1 latency-promoting gene. The effect of RYBP on HIV-1 latency was explored in multiple cell lines and primary latency models through gene knockout methods. Western blot and chromatin immunoprecipitation (ChIP) were used to explore the molecular mechanism of RYBP in promoting HIV-1 latency.

Results Disruption of RYBP gene can activate latent HIV-1 in different latent cell lines and primary latent cell models. Mechanistically, the HIV-1 long terminal repeats (LTR) region binding protein Yin Yang 1 (YY1) can recruit RYBP to the HIV-1 L region. Then, RYBP can further recruit KDM2B, thereby promoting the increased ubiquitination level of H2AK119 and decreases the level of H3K4me3, to decrease HIV-1 L transcriptional elongation and enter a latent state. At the same time, during the stage of viral transcription and replication, Tat protein can inhibit the expression of RYBP, promoting viral transcription and replication. Finally, we found that the H2AK119ub inhibitor PRT4165 can promote latent HIV-1 activation and has good synergy with reported latent reactivating agents.

Conclusion These results provide mechanistically new insights into a critical role of RYBP in the regulation of histone modification and H2AK119ub may be directly targeted to control HIV reservoirs.

Keywords RYBP, KDM2B, HIV-1 latency, H2AK119ub, EnChIP

†Xinyi Yang, Yuqi Zhu and Xiaying Zhao contributed equally to this work.

*Correspondence:
Xinyi Yang
xinyy@fudan.edu.cn
Huanzhang Zhu
hzzhu@fudan.edu.cn

Full list of author information is available at the end of the article

Background

At present, antiretroviral therapy (ART) has successfully controlled the plasma viral load below the detection line in patients [1, 2]. However, relying on ART alone cannot completely eliminate the virus in patients, mainly due to the existence of virus reservoirs [3–5]. Viral latency is established early after infection due to the persistence of transcriptionally silent HIV proviruses, predominantly in long-lived resting $CD4^+$ memory T cells [6, 7]. To eliminate the viral reservoir, the researchers proposed a "shock and kill" strategy [8]. This strategy is based on intervention the molecular mechanisms of HIV latency by therapeutically inducing viral gene and protein expression under the protection of ART and leading to selective cell death through either the lytic properties of the virus or the immune system now recognizing infected cells.

In latently infected cells, transcription of the integrated HIV-1 proviral genome is regulated by the state of its chromatin [9]. After integration into the host chromatin, two nucleosomes are precisely positioned at the HIV-1 promoter located in the 5' LTR independently from the integration site [10, 11]. Previous studies have shown that nucleosome 1, located downstream of the transcription start site, undergoes rapid remodeling during the transition between HIV-1 latency and activation states [12]. Histone methylation and deacetylation modifications have been shown to be involved in the establishment and maintenance of HIV-1 latency [13–15]. Novel histone modifications, such as histone crotonylation, have also recently been reported to be involved in the establishment and maintenance of HIV-1 latency [16].

Researchers have proved that histone deacetylase inhibitors can reverse HIV-1 latency [17]. Based on this, a number of clinical trials have been carried out, but the clinical treatment effect is not good [18, 19]. In addition, histone methylase inhibitors have also been shown to activate latent HIV-1 in in vitro cell models [20–22]. Recently, researchers also found that histone crotonylation is also involved in HIV-1 latency, and inducers against histone crotonylation also showed good latency activation in vitro [16]. In summary, the histone post-transcriptional modification plays a key role in the establishment and maintenance of HIV-1 latency, but whether there are unknown histone modifications involved in the establishment and maintenance of HIV-1 latency is still unclear.

In this study, we discovered multiple interacting proteins that can bind near the HIV-1 L region through the method of chromatin immunoprecipitation based on gene editing tools. Among them, we found that the subunit of polycomb-repressive complex 1 (PRC1)-RYBP affects the latency of HIV-1. And we found that RYBP affected the monoubiquitination of histone H2AK119 and recruited the histone demethylase KDM2B to the HIV-1 L region, which promoting H3K4me3. These epigenetic changes facilitate the establishment and maintenance of HIV-1 latency. Besides, the viral protein Tat can promote the transcription and replication of HIV-1 by inhibiting the expression of RYBP. Besides, we found that the PRC1 inhibitor, PRT4165, can promote HIV-1 latent activation by destroying H2AK119 monoubiquitination, and it has a good synergistic effect with a variety of reported latent activators.

Methods

Ethics statement

This study was approved by the Ethics Committee of School of Life Sciences(ethical approval number: FER24093R), Fudan University and the methods were consistent with the relevant guidelines and regulations of that committee. All patient samples were collected from the Shanghai Public Health Clinical Center, and samples of healthy people were collected from Shanghai Changhai Hospital. All patients and healthy donors gave informed consent for this experiment.

Cell culture

C11 cells, which were Jurkat T cells latently infected with a single provirus integrated into RNA binding protein with serine rich domain 1 gene combined with a GFP gene and under the control of the HIV-1 L, and were used as a marker of HIV-1 activation [23, 24] (constructed in our lab). J-Lat 10.6 cells, which also contained a single integrated latent HIV-GFP reporter genome, were an HIV-1 latent infection model (obtained from NIH AIDS Reagent Program). ACH2 was a clone of HIV-1 latently infected CEM cells that contained a single copy of proviral DNA per cell (obtained from NIH AIDS Reagent Program). Ya cells, which were Jurkat cells infected with a single provirus without an env gene and sustained expression of HIV-1-related viral genes in cells [23] (constructed in our lab). C11, J-Lat 10.6, ACH2, Ya, and Jurkat cells were cultured in RPMI1640 (Gibco, C11875500BT) with 10% fetal bovine serum (FBS) (Gibco, 10110154) and 1% penicillin/streptomycin (Gibco, 15140-122) in a 37 °C incubator containing 5% CO_2. 293T cells were cultured in DMEM (Gibco, C11995500BT) and supplemented with 10% fetal calf serum (ExCell Bio, FSP500), and 1% penicillin/streptomycin (Gibco) in a 37 °C incubator containing 5% CO_2.

Antibody and reagents

The following antibodies were used throughout this study: from Abclonal(Wuhan, China), anti-FLAG (AE063; 1:2500 for Western blot and 1:100 for ChIP), anti-hnRNP M(A20963; 1:1000 for Western blot), anti-HSP90AA1(A23880; 1:1000 for Western blot), anti-HMGB1(A2553, 1:1000 for Western blot), anti-CDK1

(A11420; 1:1000 for Western blot), anti-HAT-1 (A24223, 1:1000 for Western blot), anti-HSPA9 (A11256, 1:1000 for Western blot), anti-UBA2 (A17342, 1:1000 for Western blot), anti-β-Actin (AC026; 1:5000 for Western blot). From Abcam (Cambridge, UK), anti-RYBP and anti-KDM2B (ab264142; 1:1000 for Western blot). From Cell Signaling Technology (MA, USA), anti-HPF1 (47590, 1:1000 for Western blot), anti-H2AK119ub (8240, 1:100 for ChIP), anti-H3K4me3 (9751, 1:100 for ChIP). From Proteintech (Wuhan, China), HRP goat anti-mouse IgG (15014; 1:5000 for Western blot), HRP goat anti-rabbit IgG (15015; 1:5000 for Western blot). Anti-Flag Magnetic Beads (HY-K0207) was purchased from MCE. 2 × Taq Master Mix (P112), High fidelity PCR enzyme- 2 × Phanta Max Master Mix (P515) were purchased from Vazyme (Nanjing, China). PMD18-T (6011) was purchased from Takara (Beijing, China). Cell Genome Extraction Kit (DP304), Plasmid Extraction Kit (DP103, DP108, DP117) were purchased from Tiangen (Beijing, China). Gel Extraction Kit (CW2302) was purchased from CWBIO (Nanjing, China). Luciferase detection kit (E6110) was purchased from Promega (Madison, USA). Cell Counting Kit (CCK-8) and Annexin V-Alexa Fluor 488/PI apoptosis kit were purchased from Yeasen (Shanghai, China). Luciferase and nanoluc detection kit (E6110, N1110) was purchased from Promega (Madison, USA).

Construction and production of lentivirus

For production of lentivirus, HEK293T cells were seeded into 10 cm dishes one day before transfection. When the cells reached 80% confluence, plasmid and PEI (the ratio of the plasmid and PEI was 1:3) were added into the Opti-MEM (Gibco), mixed evenly, and left standing for 20 min. Indicated vector, psPAX2 and PMD2.G vector were co-transfected into HEK293T cells to produce the lentivirus. After incubation at 37 °C and 5% CO_2 for 8–12 h, the culture medium was changed with DMEM with 2% FBS and 1% P/S. The supernatants containing lentivirus were harvested at 48 h and 72 h after transfection and filtered by 0.45 μm pore size. The filtrates were centrifuged at 25,000 rpm and 4 °C for 2 h. The supernatants were discarded, and the lentivirus stocks were dissolved in Lentivirus Freezing Solution (AC04L453, Life-iLab, Shanghai) for storage at -80 °C.

EnChIP screen process

Briefly, A total of 1×10^9 C11 cells which expressed FLAG-ZFP were cross-linked with 1% formaldehyde for 10 min at room temperature and quenched with 0.125 M glycine for 5 min. After lysis, nuclear extracts were separated and chromatin was sheared by sonicator (Bioruptor UCD-200; Diagenode) for 10 min (10 s on and 10 s off) on ice to obtain DNA fragments of 200 to 1,000 bp in length. Nuclear extracts were incubated with the anti-FLAG at 4 °C overnight. Protein G/A-labeled Dynabeads were added to each sample at 4 °C for 2 h for immunoprecipitation. Afterwards, the obtained sample was decrosslinked with 5 M NaCl, and the DNA and RNA in the sample were digested by adding RNase and DNase, respectively. The remaining protein samples were concentrated by freeze-drying, identified by SDS-PAGE, and finally identified by mass spectrometry.

Vector construction

Individual sgRNA constructs targeting hnRNP M, KDM2B, RYBP, HSP90AA1, HMGB2, HAT1, HSPA9, UBA2 and HPF1 were cloned into lentiCRISPR V2 (addgene 75112). The primers were listed in Supplementary Table S2.

For cDNA expression vectors, a linearized lentiviral backbone was generated from pCMV or PCDH (Youbio, Hunan, China). Protein-coding plasmids were gifts from Professor Han Jiahuai Laboratory. All the constructed plasmids were confirmed by restriction enzyme digestion and DNA sequencing.

Cas9-mediated gene knockout and cDNA overexpression

C11, J-Lat 10.6 and ACH2 cells were infected with lentivirus at an MOI of 1 and then selected with 2 μg/ml puromycin for 14 days. The knockout and the overexpression were detected by Western blot (WB) analysis. For gene knockout in rKDM2B cell line, we transfected the px330 plasmid targeting YY1 or RYBP by electrotransfection, then sorted monoclonal cells and identified the knockout cells by Western blot.

Visualization of GFP and flow cytometry assay

Green fluorescent protein (GFP), a marker for the activation of HIV-1 in infected cells, was visualized by fluorescence microscopy after cell sorting. The cells were collected and washed with phosphate buffered saline (PBS). Cells were kept in PBS before analysis on a BD LSRII flow cytometer for enhanced GFP expression. FlowJo software (FlowJo LLC, Ashland, OR) was used to perform the flow cytometry analysis.

Enzyme-linked immunosorbent assay (ELISA) detection of antigen p24 levels

ACH2 cells were each seeded at a density of 1×10^6 on a 6-well plate. After 48 h of culture, HIV-1 production was measured via quantification of p24 in culture supernatant using p24 ELISA kit (R&D System, Minnesota, USA).

ChIP experiments

ChIP experiments were performed according to protocol provided by EZ-ChIP chromatin immunoprecipitation kit (Millipore). Briefly, 1×10^7 cells were cross-linked

with 1% formaldehyde for 10 min at room temperature and quenched with 0.125 M glycine for 5 min. After lysis, nuclear extracts were separated and chromatin was sheared by sonicator (Bioruptor UCD-200; Diagenode) for 10 min (10 s on and 10 s off) on ice to obtain DNA fragments of 200 to 1,000 bp in length. 1% of total sheared chromatin DNA was used as the input. Nuclear extracts were incubated with the indicated antibodies at 4 °C overnight. Protein G/A-labeled Dynabeads were added to each sample at 4 °C for 2 h for immunoprecipitation. The immunoprecipitated DNA was analyzed by real-time PCR with Hieff qPCR SYBR Green Master Mix (11201ES, Yeasen, Shanghai). Specific primers for qRT-PCR are designed according to PrimerBank and listed in Supplementary Table S2.

Western blot

A total of 1×10^6 cells were seeded in a 10-cm dish and cultured for 24 h. Then, the cells were harvested, lysed, and subjected to Western blot. Membranes were visualized using the Omni-ECL™ Chemiluminescence Kit (SQ230L, Epizyme biotech, Shanghai) and images were captured using the ChemiDoc XRS + System and processed using ImageLab software (Bio-Rad).

Isolation of primary CD4$^+$ T cells

Peripheral blood mononuclear cells (PBMCs) isolated from healthy donors were purchased from the Changhai Hospital of Naval Medical University (Shanghai, China). Naive CD4$^+$ T cells were further purified from peripheral blood mononuclear cells by negative selection according to the manufacturer's instructions (Thermo). The Naive CD4$^+$ T cells were maintained in serum-free medium supplemented with 1% penicillin-streptomycin and 5 ng/ml recombinant human IL-2 (C013, novoprotein, Shanghai) and 10 ng/ml IL-7 (C086, novoprotein, Shanghai) at 37 °C in 5% CO_2.

Cell proliferation by CCK-8 assay

Cells differently treated were seeded at a density of 0.5×10^4 on 96-well plate. 10% CCK-8 solution was added to fresh culture medium. The cells were incubated at 37 °C for 1 h. The OD 450 nm value was measured to determine cell proliferation.

Apoptosis detected by Annexin V-Alexa fluor 488/PI staining

A total of 1×10^6 cells were collected in a 1.5 ml tube and centrifuged at 300 g for 5 min. The cells were washed twice with 500 µl PBS and analyzed with Annexin V-Alexa Fluor 488/PI apoptosis detection kit according to the manufacturer's instructions. The proportion of Annexin V-Alexa Fluor 488-positive cells was assayed by flow cytometer and analyzed by FlowJo software (FlowJo LLC, Ashland, OR).

Extraction of total RNA, reverse transcription, and qRT-PCR

Total RNA was extracted from cells using TRIzol reagent (Invitrogen, USA) following the manufacturer's instructions or obtained by RIP experiment. cDNA was synthesized by reverse transcription using a BeyoRT™ III cDNA Synthetic premix. (Beyotime, China). qRT-PCR was then performed on an Applied Biosystems 7500 Real Time PCR System (Thermo Fisher Scientific, USA) using a reaction mixture consisting of 5 µL Hieff qPCR SYBR Green Master Mix (11201ES, Yeasen, Shanghai). GAPDH was used as an internal reference for mRNA. Specific primers for qRT-PCR are designed according to PrimerBank and listed in Supplementary Table S2.

Quantitative analysis of latency-reversing agent combinations

We used the Bliss independence model as a metric to evaluate the latency-reversing activity of drug combinations [25]. This model is defined by the equation:

$$fa_{xy}\,, P = fa_x + fa_y - (fa_x)(fa_y) \tag{1}$$

where fa_{xy},P is the predicted fraction affected by a combination of drug x and drug y, given the experimentally observed fraction affected by treatment with drug x (fa_x) or drug y (fa_y) individually. The experimentally observed fraction affected by a combination of drug x and drug y (fa_{xy},O) can be compared with the predicted fraction affected, which is computed using the Bliss model (fa_{xy},P) as follows:

$$\Delta\, fa_{xy} = fa_{xy}\,, O - fa_{xy}\,, P \tag{2}$$

If $\Delta fa_{xy}>0$ with statistical significance, then the combined effect of the two drugs exceeds that predicted by the Bliss model and the drug combination displays synergy. If $\Delta fa_{xy}=0$, then the drug combination follows the Bliss model for independent action. If $\Delta fa_{xy}<0$ with statistical significance, then the combined effect of the two drugs is less than that predicted by the Bliss model and the drug combination displays antagonism. In our analysis, the fraction affected was calculated as follows for the percentage of GFP-positive cells: fa_x=% GFP-positive cells after treatment with drug x-% GFP-positive cells treated with the DMSO control.

Statistical analysis

Data are representative of three independent experiments, and error bars represent standard errors (SD). Paired samples t-tests were performed with use of SPSS version 13.0 (SPSS Inc., Chicago), and statistical

significance was indicated at $^{*}p<0.05$, $^{**}p<0.01$ or $^{***}p<0.001$.

Results

Candidate proteins interacting with the latent HIV-1 L region were obtained by enchip

Since it is still unclear whether there are new and unknown proteins that promote HIV-1 latency in the HIV-1 L region, the key site of HIV-1 latent activation, we tried to use the latest gene editing-based enChIP technology to explore the potential of proteins that interact with the HIV-1 L region (Fig. 1A). Briefly, to obtain interacting proteins that specifically bind to the DNA fragment of interest, editing tool enzymes, such as ZFP, dCas9, etc., which are tagged and capable of binding to the DNA fragment of interest, were expressed in cells.

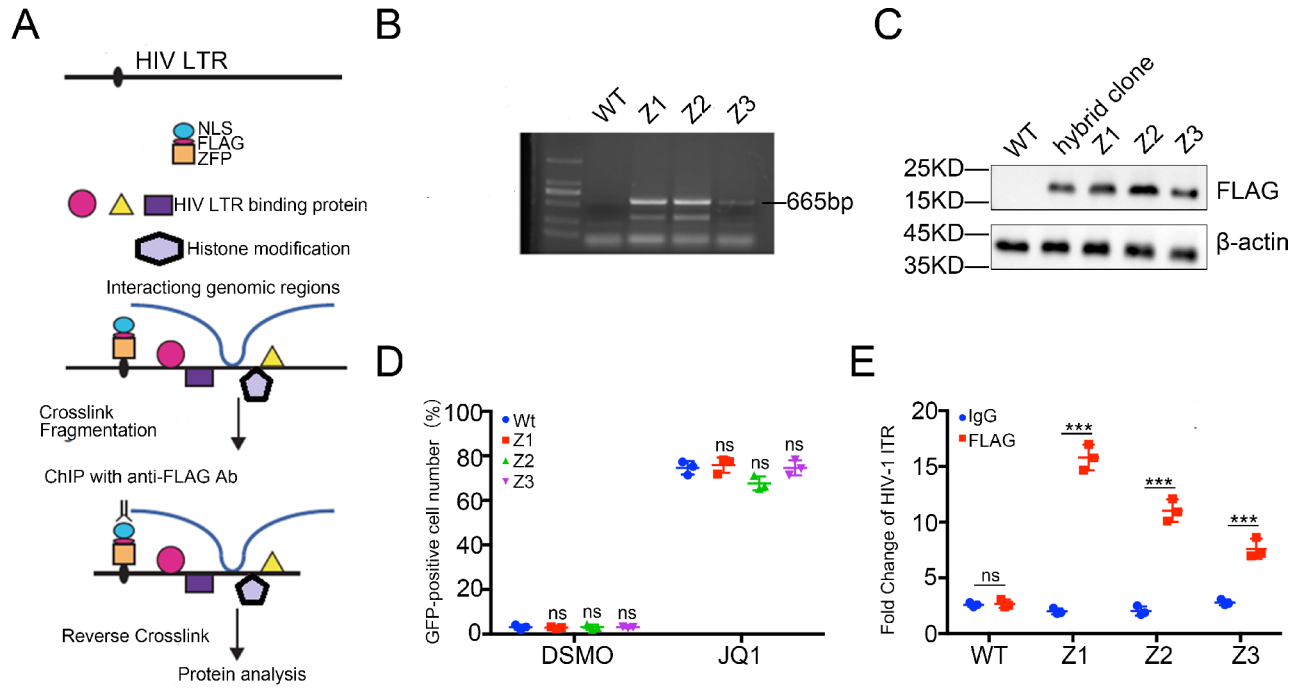

F

Bait:FLAG-ZFP3			
Known protein		Unknown protein	
HDAC2	36	HnRNP M	39
HMGB1	33	KDM2B	29
HnRNP A2B1	32	RYBP	23
IFI16	25	HSP90AA1	22
LSD1	22	HMGB2	21
LEF1	21	CDK1	19
NF-kB	19	HAT-1	18
NAT10	15	HSPA9	18
RUNX1	12	UBA2	18
SP-1	9	HPF1	17

Fig. 1 Systematic identification of HIV-1 L interacting proteins using enChIP. (**A**) Schematic representation of the enChIP. (**B**) By extracting the genomes of cells in different monoclonal latent cell lines and using specific primers targeting FLAG-ZFP for PCR identification, it was verified that the FLAG-ZFP was stably integrated into the infected group cells. WT, wild type. (**C**) Western blot of cell lysate with anti-FLAG antibody was performed to identify the expression of FLAG-ZFP protein in different monoclonal latent cell lines. (**D**) The effect of FLAG-ZFP on the latency state and activation of HIV-1 in different monoclonal latent cell lines. The BET inhibitor JQ1 (0.1 μM) is used as a latency activator to assess whether FLAG-ZFP affects the latency activation of HIV-1. The percentage of GFP-positive cells was measured by flow cytometry to determine the level of HIV-1 reactivation. Each data represented the mean ± SD of three independent experiments ($n=3$) and were analyzed with T-test compared with WT cells. ns, $p>0.05$. (**E**) The interaction between FLAG-ZFP with HIV-1 L was detected by ChIP. Chromatin fragments from different monoclonal latent cell lines were immunoprecipitated with anti-FLAG antibodies or control normal rabbit serum (IgG). After ChIP, the binding of FLAG-ZFP into HIV LTR was detected by qPCR with specific primers for HIV LTR. The number of copies was normalized to input group. Each data represented the mean ± SD of three independent experiments ($n=3$) and were analyzed with T-test compared with IgG. ns, $p>0.05$ ***, $p<0.001$. (**F**) The number of total peptides identified by mass spectrometry analysis with FLAG-ZFP as bait. Top ten most abundant proteins that have been reported and not reported to interact with the HIV-1 L region

After fixation with formaldehyde, the ChIP experiment is conducted using tag antibodies such as FLAG. Following the acquisition of the DNA/protein interaction mixture, the DNA fragments are digested with DNase. Then the retained proteins are identified via mass spectrometry to obtain potential interacting proteins (Fig. 1A). Therefore, in order to perform enChIP experiments in latently infected cells, we first overexpressed a zinc finger protein targeted the HIV-1 L region [26] in the latently infected cell line C11, which was previously established in our laboratory [23, 24]. Three different monoclonal cell lines were obtained by infinite dilution method. In order to confirm whether the monoclonal cell lines integrate and express FLAG-tagged zinc finger proteins (FLAG-ZFP), we verified them at the genomic and protein levels by polymerase chain reaction (PCR) and Western blot, respectively. The results showed that the monoclonal Z1, Z2 and Z3 all had FLAG-ZFP genes integrated (Fig. 1B), and Z1, Z2 and Z3 all stably expressed FLAG-ZFP protein (Fig. 1C). Afterwards, we treated Z1, Z2 and Z3 cells with or without the addition of the latent activator JQ1 and found that stable expression of FLAG-ZFP did not affect HIV-1 latency and activation (Fig. 1D). Afterwards, we confirmed that FLAG-ZFP could interact with HIV-1 L region in Z1, Z2 and Z3 cloned cells by ChIP experiments (Fig. 1E).

The above results demonstrate that we have successfully obtained engineered cell lines capable of enChIP. Afterwards, we performed enChIP experiments in Z1 monoclonal cell line by anti-FLAG and obtained potential candidate proteins that interact with HIV-1 L region. Finally, we subjected PAGE gels containing candidate proteins to mass spectrometry identification. We found that we obtained the reported proteins interacting with the HIV-1 L region, including HDAC2 [27], HMGB1 [28], SP-1 [29], NF-kB [30], etc., which further confirmed the reliability of our experimental results. Besides, we also found some potential candidate proteins related to HIV-1 L region, such as hnRNP M, KDM2B, RYBP, CDK1 and HAT-1, have not been reported yet (Fig. 1F). Therefore, in follow-up studies, we will focus on these previously unreported candidate proteins related to HIV-1 latency.

RYBP and KDM2B promote HIV-1 latency

To further verify whether the candidate proteins obtained by enChIP are involved in HIV-1 latency, we used CRISPR/Cas9 technology to knock out the above candidate genes in the latently infected cell line C11 and J-Lat 10.6 and detected the activation of latent HIV-1 by flow cytometry. The results showed that knockout of KDM2B and RYBP could promote HIV-1 latent activation (Fig. 2A and B). And we confirmed the knockout efficiency of the candidate gene through Western blot (Supplementary Fig. S1). Afterwards, we further verified the effect of knockout KDM2B and RYBP on HVI-1 latency in the true virus latent cell line ACH2. And we found that the p24 viral protein secreted by ACH2 knocked out of KDM2B or RYBP was significantly increased by anti-p24 ELISA (Fig. 2C). Then, we confirmed the knockout of KDM2B or RYBP in ACH2 cells by western blot (Fig. 2D). To exclude potential off-target effects, we complemented the corresponding candidate genes in C11 cells with RYBP or KDM2B knockout and assessed the activation of HIV-1 latency through flow cytometry. The results indicated that the activation level of HIV-1 was suppressed to around the baseline level (Fig. 2E and F). To investigate whether enhancing RYBP or KDM2B could inhibit HIV-1 expression, we also overexpressed KDM2B or RYBP in the Ya cell line integrating and continuously expressing the HIV-1 pseudoviral genome with the GFP reporter gene [24, 25]. As a result, we found that either overexpression of KDM2B or RYBP could significantly inhibit the expression of GFP in Ya cells (about 25% and 35%, respectively). However, the overexpression of FLAG-KDM2B was less effective in suppressing HIV-1 expression compared to the overexpression of FLAG-RYBP (Fig. 2G and H). Finally, by targeting different sites of HIV-1 mRNA and utilizing qPCR, we investigated whether RYBP and KDM2B influence the initiation or elongation of HIV-1 transcription. The results revealed that both RYBP and KDM2B primarily exert their influence on the transcriptional elongation phase of HIV-1 (Supplementary Fig. S2). In summary, these results further confirm that KDM2B and RYBP are indeed involved in latency.

RYBP binds to the HIV-1 L region through YY1 and recruits KDM2B

RYBP and KDM2B are proteins involved in epigenetic modification, the epigenetic modification of the HIV-1 L region is a key factor in the establishment of HIV-1 latency [31]. Therefore, we want to further explore whether KDM2B and RYBP regulate HIV-1 latency by directly interacting with the HIV-1 L region, or indirectly affect HIV-1 latency by participating in upstream signaling pathways. Considering that there is currently a lack of KDM2B-targeting antibodies that can be used for ChIP or co-immunoprecipitation, we utilized the cell line in which FLAG-KDM2B was complemented in the C11-KDM2B-KO cell line for subsequent studies. (namely rKDM2B cells) (Fig. 3A). Then, we firstly conducted ChIP experiments with anti-RYBP or anti-FLAG in rKDM2B cells. We found that RYBP and FLAG-KDM2B can be significantly enriched to DNA fragments in the HIV-1 L region (Fig. 3B), which suggests that either KDM2B or RYBP regulates HIV-1 latency by binding to the HIV-1 L region. After that, we found that RYBP may

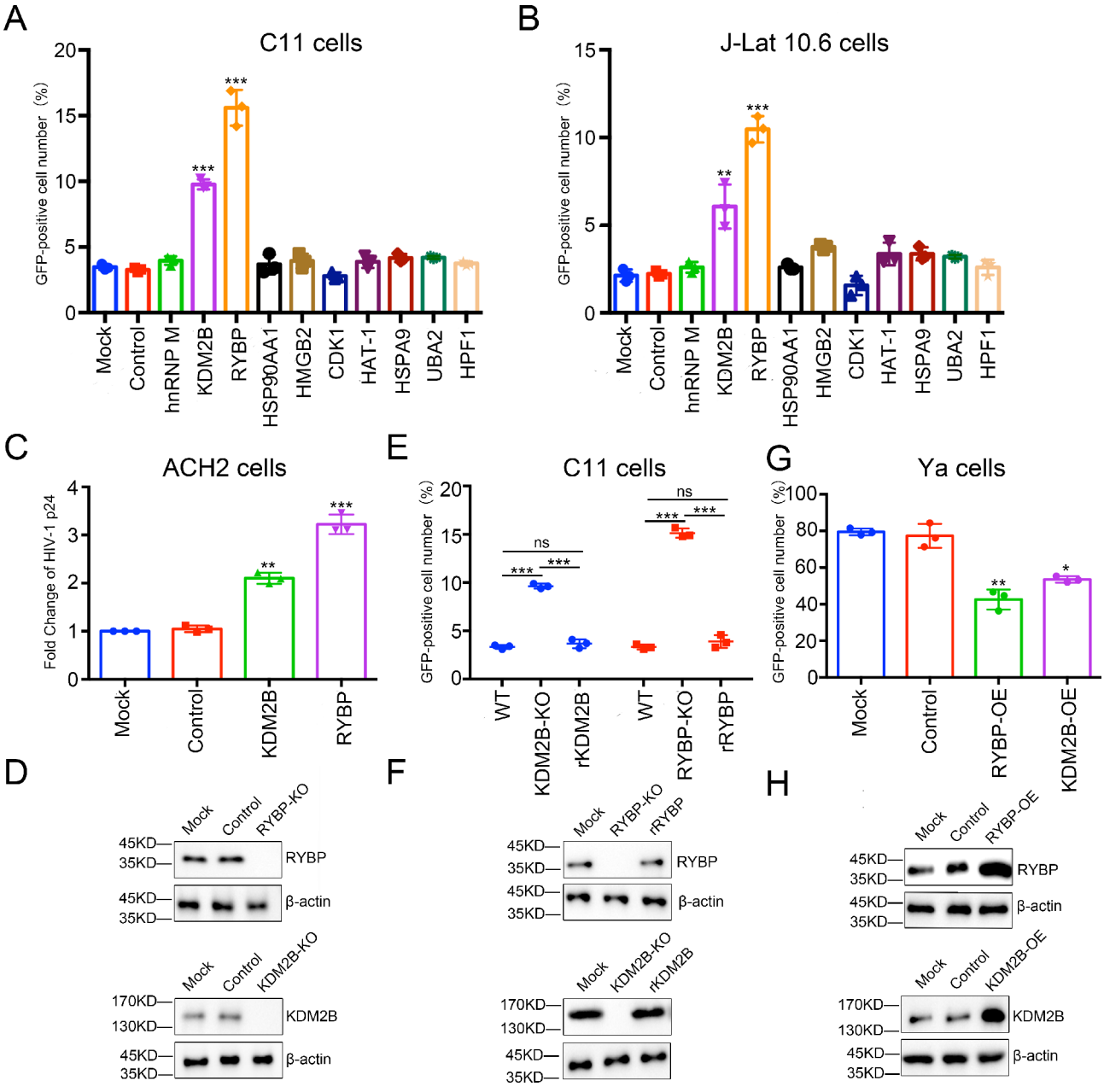

Fig. 2 Validation of the candidate genes screened from the enChIP. (**A**, **B**) Knockout the top 10 gene in C11 and J-Lat 10.6 cell line. C11 and J-Lat 10.6 cell lines were infected by lentiCRISPR v2.0 packaged lentiviruses with sgRNA following by screening for 14 days with purinomycin 2 μg/ml. The percentage of GFP-positive cells was measured by flow cytometry to determine the level of HIV-1 reactivation. (**C**) The effect of knocking out the *RYBP or KDM2B* gene on HIV latency was further verified in ACH2 models of HIV latency. The expression levels of p24 in ACH2 cells was detected by HIV-1 p24 ELISA. (**D**) Western blot of cell lysate with anti-RYBP or anti-KDM2B antibody was performed to identify the expression of RYBP or KDM2B protein in different ACH2 cell lines. (**E**) The effect of back complementated of RYBP or KDM2B on HIV-1 latency in different C11 cell lines. The percentage of GFP-positive cells was measured by flow cytometry to determine the level of HIV-1 reactivation. (**F**) Western blot of cell lysate with anti-RYBP or anti-KDM2B antibody was performed to identify the expression of RYBP or KDM2B protein in different C11 cell lines. (**G**) The effect of overexpression the RYBP or KDM2B on HIV was further verified in Ya cell line. The percentage of GFP-positive cells was measured by flow cytometry to determine the level of HIV-1 expression. (**H**) Western blot of cell lysate with anti-RYBP or anti-KDM2B antibody was performed to identify the expression of RYBP or KDM2B protein in different Ya cell lines. Mock, untreatment, Control, treatment with empty lentivirus. Each data represented the mean ± SD of three independent experiments ($n = 3$) and were analyzed with T-test compared with mock cells. *, $p < 0.05$, **, $p < 0.05$, ***, $p < 0.001$

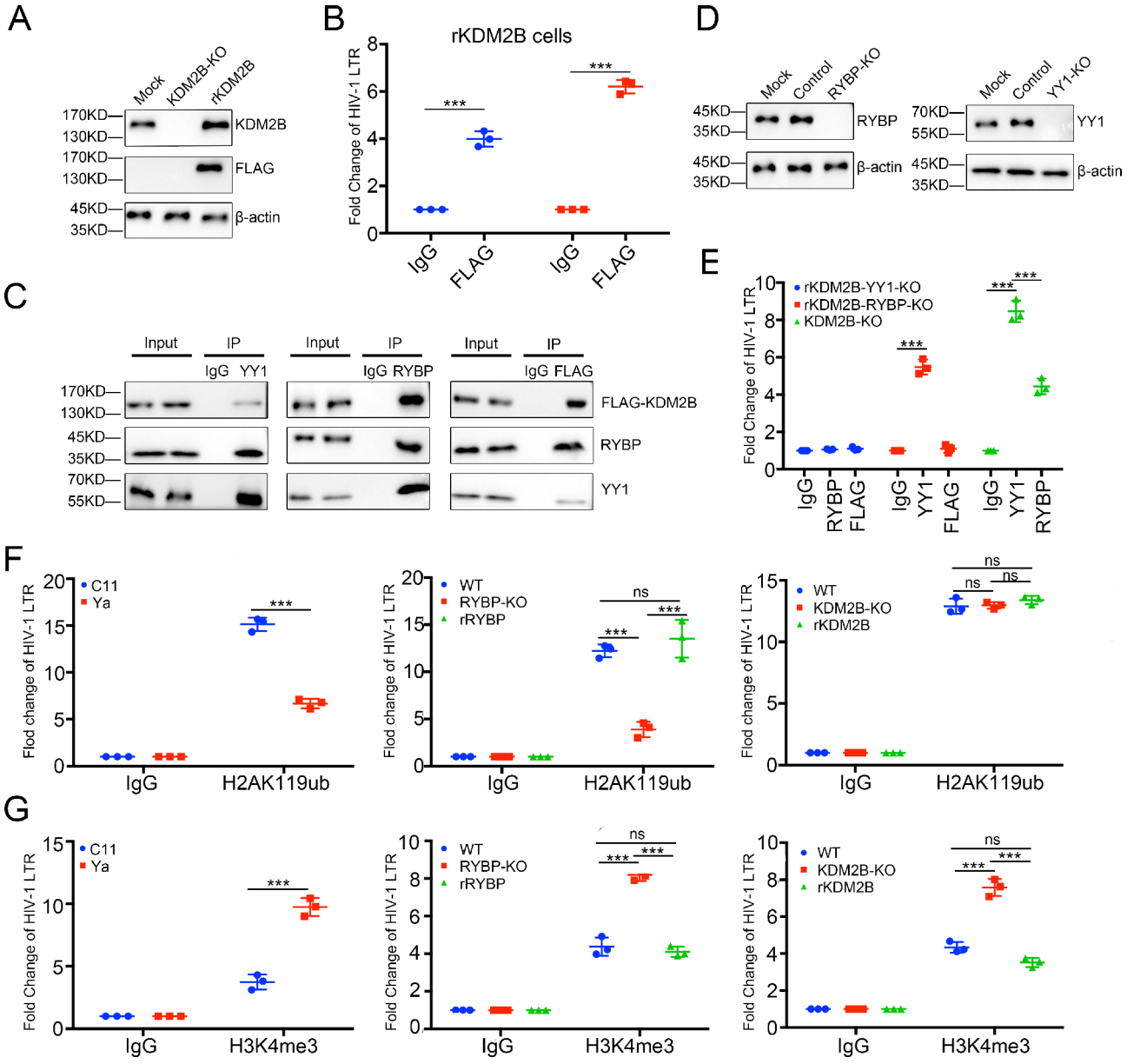

Fig. 3 RYBP and KDM2B promote HIV-1 latency by binding to the HIV-1 L and change the level histone modification.(**A**)KDM2B protein levels were measured by Western blotting in C11, C11-KDM2B-KO and C11-rFLAG-KDM2B with anti-KDM2B or anti-FLAG.(**B**)The interaction between RYBP and FLAG-KDM2B with HIV-1 L was detected by ChIP. Chromatin fragments from C11-FLAG-rKDM2B cells was immunoprecipitated with anti-FLAG or anti-RYBP or control normal rabbit serum (IgG). After ChIP, the binding of RYBP and FLAG-KDM2B into HIV LTR was detected by qPCR with specific primers for HIV LTR. (**C**) The immunoprecipitation assay was performed in C11-FLAG-rKDM2B cells lysates with anti-YY1, anti-RYBP or anti-FLAG followed by Western blot with anti-YY1, anti-RYBP or anti-KDM2B. (**D**) YY1 and RYBP protein levels were measured by Western blotting in C11-FLAG-rKDM2B cells after knockout YY1 or RYBP. (**E**) The direct or indirect interaction between RYBP and KDM2B with HIV-1 L was detected by ChIP. Chromatin fragments from C11-FLAG-rKDM2B cells which was knocked out YY1 or RYBP, and C11-KDM2B-KO cells were immunoprecipitated with anti-YY1, anti-RYBP, anti-FLAG or control normal rabbit serum (IgG). After ChIP, the binding of YY1, RYBP and FLAG-KDM2B with HIV LTR was detected by qPCR with specific primers for HIV LTR. (**F**, **G**)The H3K4me3 and H2AK119ub level of the HIV-1 L region was detected by ChIP in C11 and Ya cells. Chromatin fragments from C11 or Ya cells were immunoprecipitated with anti-H3K4me3, anti-H2AK119ub or control normal rabbit serum (IgG). After ChIP, the H3K4me3 and H2AK119ub level was detected by qPCR with specific primers for HIV LTR. (**H-K**) The H3K4me3 and H2AK119ub level of the HIV-1 L region was detected by ChIP. Chromatin fragments from C11, C11-RYBP-KO, C11-rRYBP (**H**, **I**) or C11 and C11-KDM2B-KO, C11-rKDM2B (**J**, **K**) cells were immunoprecipitated with anti-H3K4me3, anti-H2AK119ub or control normal rabbit serum (IgG). After ChIP, the H3K4me3 and H2AK119ub level was detected by qPCR with specific primers for HIV LTR. Mock, untreatment; control, treatment with empty lentivirus or plasmid. Each data represented the mean ± SD of three independent experiments ($n = 3$) and were analyzed with T-test compared with mock cells. *, $p < 0.05$, **, $p < 0.05$, ***, $p < 0.001$

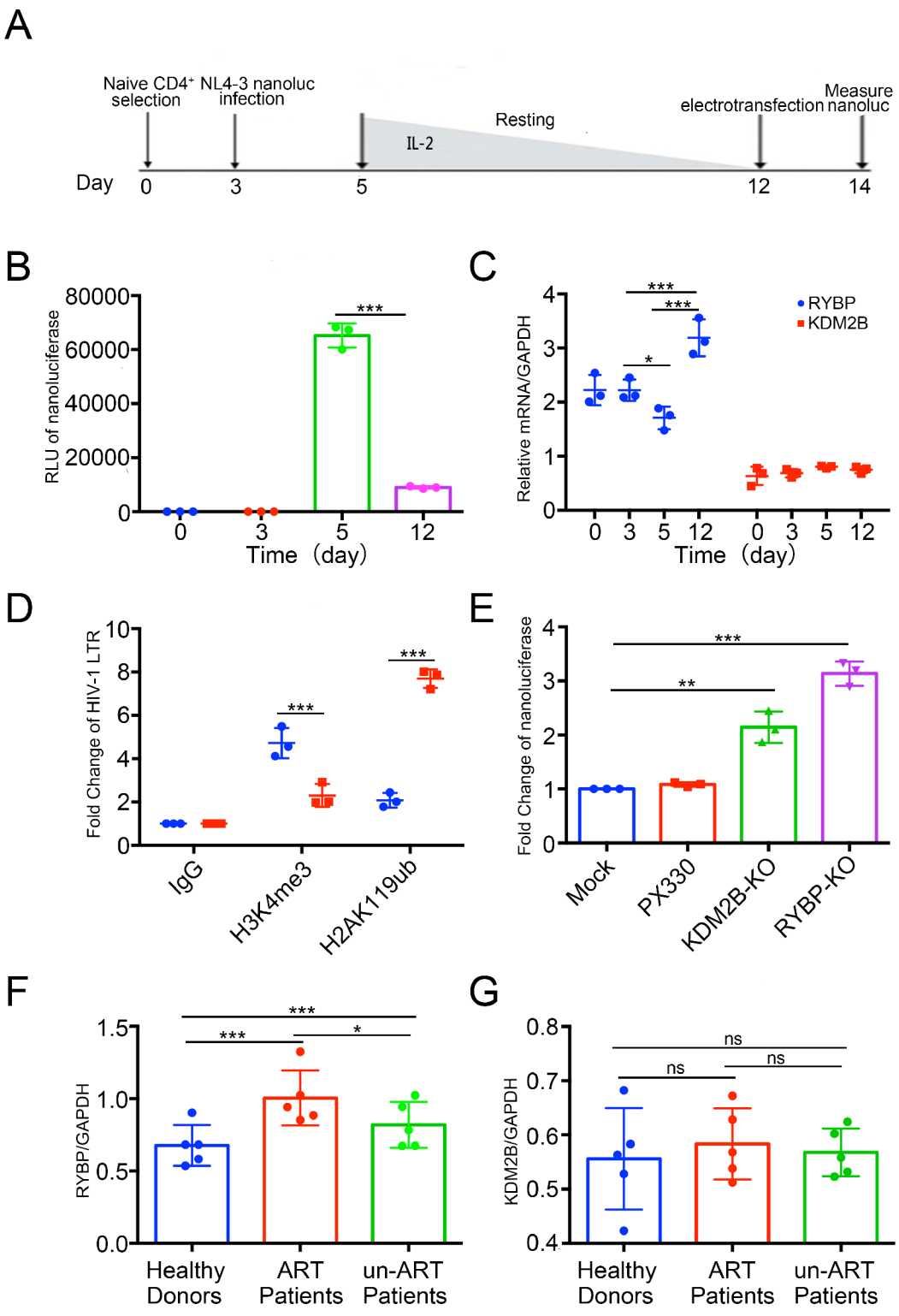

Fig. 4 (See legend on next page.)

interact with KDM2B through the mass spectrometry database. In addition, RYBP may also interact with YY1, a transcription factor that has been reported to be related to HIV-1 latency [32]. Therefore, we further explored the interaction of YY1, FLAG-KDM2B and RYBP by co-immunoprecipitation in rKDM2B cells. The results showed that RYBP not only interacted with YY1 protein, but also had significant interaction with FLAG-KDM2B.

(See figure on previous page.)

Fig. 4 The effect of RYBP and KDM2B on HIV-1 latency primary cell models and patient cells. (**A**) The outline of latency establishment in the primary $CD4^+$ T cells. Human primary $CD4^+$ T cells were activated and expanded with α-CD3/CD28 beads at day 1. The α-CD3/CD28 beads were removed at day 3. Cells were then infected with HIV-1 NL4.3-nanoluciferase at 3rd day after expansion and maintained over 7 days with a decreasing concentration of IL-2 to establish latency until day 12. At day 12, cells were transfected with PX330, PX330-RYBP-sgRNA/Cas9 or PX330-KDM2B-sgRNA/Cas9 by electrotransfection. (**B**) The transcription of HIV-1 in the primary $CD4^+$ T cells was determined by nanoluciferase assays during HIV-1 infection (total 5×10^5 cells). (**C**) After infecting with VSV-G-pseudotyped HIV-1 NL4.3-nanoluciferase, the mRNA expression of RYBP and KDM2B were measured by qPCR at different time. (**D**) After infecting with VSV-G-pseudotyped HIV-1 NL4.3-nanoluciferase, the H3K4me3 and H2AK119ub level of the HIV-1 L region were detected by ChIP at different time as mentioned before. (**E**) The role of RYBP and KDM2B in the primary latency model. The expression of HIV-1 was measured by nanoluciferase in the primary $CD4^+$T cells after gene knockout by Mock, PX330, PX330-RYBP-KO or PX330-KDM2B-KO with electroporation. (**F**, **G**) The mRNA expression of RYBP and KDM2B in primary $CD4^+$T cells isolated from healthy donors ($n = 5$), un-ART patients ($n = 5$) and ART patients ($n = 5$) were measured by qPCR. Each data represented the mean ± SD of three independent experiments ($n = 3$) and were analyzed with T-test. *, $p < 0.05$, **, $p < 0.05$, ***, $p < 0.001$

In addition, FLAG-KDM2B can also interact with RYBP or YY1, and YY1 also has the same effect (Fig. 3C). Later, in order to explore the interaction between the YY1, FLAG-KDM2B, RYBP and HIV-1 L, we constructed RYBP-KO or YY1-KO cell lines in rKDM2B cells by electrotransfecting PX330 plasmid targeting YY1 or RYBP knockout (Fig. 3D). Then, we found that when the YY1 protein was deleted, neither FLAG-KDM2B nor RYBP could bind to the HIV-1 L region. Deletion of RYBP only resulted in no longer interaction between FLAG-KDM2B and the HIV-1 L region. Deletion of KDM2B does not affect the interaction of RYBP with YY1 and HIV-1 L (Fig. 3E). These results indicate that RYBP binds to the HIV-1 L region through YY1 and recruits KDM2B to also reach this region.

RYBP and KDM2B promote HIV-1 latency by affecting histone epigenetic modification in the HIV-1 L region

In previous studies, the researchers had identified KDM2B as a histone demethylase involved in the demethylation of H3K4me3 [33]. As the core component of the PRC1, RYBP can participate in the monoubiquitination of histone H2AK119 [34]. Therefore, we first investigated the methylation level of H3K4me3 and the monoubiquitination level of H2AK119 in C11 and Ya cells. As a result, we found that the methylation level of H3K4me3 was significantly decreased and the monoubiquitination level of H2AK119 was significantly increased in the C11 cell line compared with the Ya cell line (Fig. 3F and G). These results showed that H3K4me3 methylation promotes latent HIV-1 activation, while H2AK119 monoubiquitination promotes HIV-1 latency. After that, we detected the changes of H3K4me3 methylation and H2AK119 monoubiquitination in the RYBP knockout C11 cells. We found that when RYBP was knocked out, H2AK119 monoubiquitination levels were significantly decreased, while H3K4me3 methylation levels were significantly increased (Fig. 3G and H). However, when KDM2B was knockout in C11 cells, the methylation level of H3K4me3 was significantly increased, H2AK119 monoubiquitination levels did not change (Fig. 3I and J). To exclude potential errors caused by off-target effects of RYBP or KDM2B knockout, we repeated the experiments using the previously established complemented cell lines. The results showed that the effects induced by the knockout were reversed upon complementation with RYBP or FLAG-KDM2B, thereby ruling out potential off-target effects (Fig. 3G and I). Meanwhile, we also examined other histone modifications involved in HIV-1 latency, such as H3K27ac and H3K9me3 [29, 35]. The results revealed that although the knockout of RYBP or KDM2B had a slight impact on the modification levels of H3K27ac and H3K9me3, there was no statistically significant difference. These finding further confirm that RYBP or KDM2B primarily influences HIV-1 latency by altering the modification levels of H2AK119ub and H3K4me3 (Supplementary Fig. S3). In summary, the results illustrates that RYBP not only affects the epigenetic modification near the HIV-1 L region by itself, but also further promotes epigenetic silencing by recruiting KDM2B.

The effection of RYBP and KDM2B in primary HIV-1 latent cell models and patient samples

Considering that there are significant differences between cell lines and primary cells, we considered further exploring the role of RYBP and KDM2B on HIV-1 latency by constructing a primary HIV-1 latent cell model as mentioned before [29] (Fig. 4A). At different time points, we detected the expression level of nanoluciferase to prove that the virus entered the latent state in the primary latency model we constructed (Fig. 4B). Besides, we detected the mRNA changes of RYBP and KDM2B and found that when NL4-3-nanoluciferase just infected primary $CD4^+$ T lymphocytes (equivalent to the acute infection period), the expression level of RYBP decreased significantly, but KDM2B did not change significantly. After that, as the concentration of IL-2 gradually decreased, the HIV-1 pseudovirus in the primary $CD4^+$ T lymphocytes gradually entered into a latent state over time. During this process, we found that the expression of RYBP gradually increased (Fig. 4C). Considering the changes in IL-2 concentration during the construction of the latent model, we simultaneously detected the mRNA levels of RYBP and KDM2B in $CD4^+$T cells that were not infected with HIV-1 pseudovirus. We found that the mRNA levels of RYBP and KDM2B were not influenced

by the concentration of IL-2 (Supplementary Fig. S4). These results suggest that there is a negative correlation between the expression level of RYBP and the expression level of the HIV-1. Then, we further examined the levels of H3K4me3 and H2AK119ub near the HIV-1 L. We found that the results in primary models were consistent with those in cell lines (Fig. 4D). At the same time, after HIV-1 entered the latent state on day 12, we transfected the latency cells with plasmid targeting knockout of RYBP or KDM2B through electroporation. On day 14, we detected the expression level of nanoluciferase and found that whether knockout of RYBP or KDM2B could significantly promote latent HIV-1 activation (Fig. 4E), which further supports the conclusions we obtained in the cell lines.

Finally, considering that there are still some differences between the primary latent model and real patient samples, we decided to detect the expression of RYBP and KDM2B in patient samples. We compared the expression levels of RYBP and KDM2B in $CD4^+$ T lymphocytes in peripheral blood among five un-ART patients, which were untreated with ART patients, ART treated patients and five healthy donors (Supplementary Table S1). The results showed that the expression levels of RYBP in patients receiving ART was higher than that in healthy people and the expression levels of RYBP in un-ART treatment patients was lower than that in healthy people (Fig. 4F). However, there was no significant difference in the expression of KDM2B between patients receiving ART treatment and un-ART treatment compared with healthy donors (Fig. 4G). The above results indicate that RYBP is also negatively correlated with HIV-1 transcription in patients.

HIV-1 viral protein Tat inhibits RYBP expression

Considering that during the establishment of the primary HIV-1 latent model, we found that the expression level of RYBP decreased significantly during acute infection. So, we first detected differences in the mRNA levels of RYBP and KDM2B in cell lines of different states. We found that in Ya cells with persistent HIV-1 expression, the expression level of RYBP was significantly lower than that of latently infected C11 cells and the parent cell line Jurkat, but there was no significant difference in KDM2B (Fig. 5A and B). These results suggested that there may be a certain viral protein that inhibits RYBP and thereby promotes HIV-1 replication. Then, we decided to further explore which viral protein would inhibit the expression

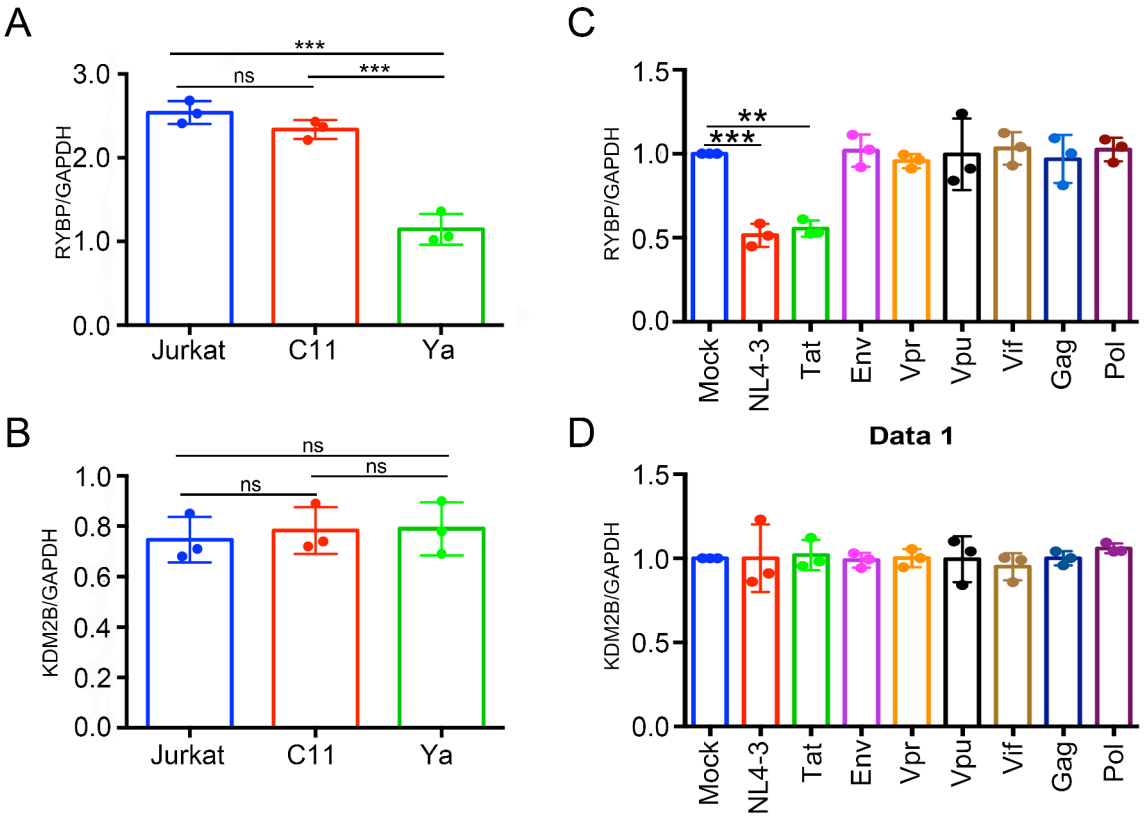

Fig. 5 HIV-1 Tat inhibits the expression of RYBP. (**A**, **B**) Expression levels of RYBP and KDM2B in different HIV-1 states. RYBP and KDM2B mRNA levels were measured by qPCR in C11, Ya and Jurkat cells. (**C**, **D**) Effect of HIV-1 viral proteins on RYBP and KDM2B expression. Each data represented the mean ± SD of three independent experiments ($n = 3$) and were analyzed with T-test. *, $p < 0.05$, **, $p < 0.05$, ***, $p < 0.001$

of RYBP. We transfected different viral protein expression plasmids into 293T cells, including Tat, Rev, Vif, Vpu, Env, Gag, Pol, we found that when we transfected the plasmid that expressed Tat protein, the expression of RYBP decreased significantly by qPCR. However, no viral protein affects the expression of KDM2B (Fig. 5C and D), which is consistent with the results of the primary model. So, to determine whether the Tat protein directly inhibits the transcriptional activity of the RYBP promoter, we conducted a ChIP assay targeting the RYBP promoter region. To explore whether Tat could bind to the RYBP promoter. The results revealed that the Tat protein was unable to bind to the promoter region of RYBP (Supplementary Fig. S5), indicating that Tat's inhibition of RYBP transcription may be mediated by influencing other proteins or pathways, thereby affecting RYBP.

PRT4165 promotes HIV-1 activation in HIV-1 cell lines and primary CD4$^+$T HIV−1 latent cell model

Considering the important role of RYBP in promoting HIV-1 latency, and that RYBP is a core component of the PRC1 [33], which is critical for histone H2AK119 monoubiquitination. Therefore, we considered to further explore the effect of PRT4165, a small molecule inhibitor against PRC1 complex and H2AK119 monoubiquitination [36], on HIV-1 latency. We first treated with different concentrations of PRT4165 for 24 h in C11 and J-lat 10.6 cell line, and found that PRT4165 can not only activate the C11 and J-Lat 10.6 cells, but also in a concentration-dependent manner. However, compared with the positive control drug JQ1, the activation efficiency and EC of PRT4165 were lower (Fig. 6A and B). Afterwards, we repeated the above experiments in the true virus latent cell line ACH2 and obtained similar results (Fig. 6C). in

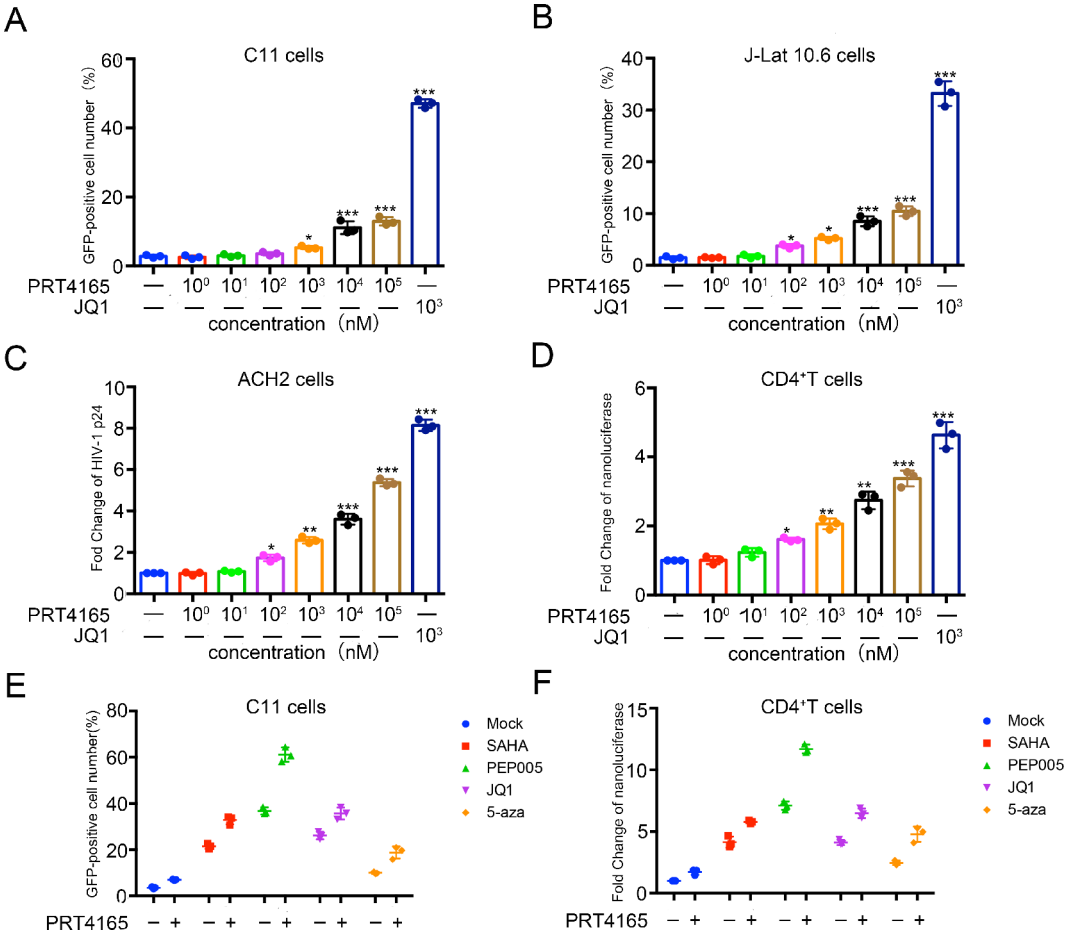

Fig. 6 PRT4165 promotes HIV-1 activation in HIV-1 cell lines and primary CD4$^+$T HIV−1 latent cell model. (**A**, **B**) C11 and J-Lat 10.6 cells were treated with different concentrations of PRT4165 for 48 h and GFP, representing the level of HIV-1 transcription, was measured by flow cytometry. (**C**) ACH2 cells were treated with different concentrations PRT4165 for 48 h and the HIV-1 p24, representing the level of HIV-1 transcription, was measured by ELISA. (**D**) Primary CD4$^+$T HIV−1 latent cells were untreated with different concentrations PRT4165 for 48 h. The effect of activation of the HIV-1 promoter was determined by nanoluciferase. (**E**, **F**) C11 and Primary CD4$^+$T HIV−1 latent cells were treated with DMSO, SAHA (0.50 μM), PEP005 (0.01 μM), JQ1 (0.01 μM) or 5-aza (1 μM) alone or with either PRT4165 (10 μM), respectively. The effect of activation of the latent HIV-1 was determined by flow cytometry (**E**) or the level of nanoluciferase (**F**) at 48 h after treatment. Mock, cells treated with DMSO. Each data represented the mean ± SD of three independent experiments ($n = 3$) and were analyzed with T-test. *, $p < 0.05$, **, $p < 0.05$, ***, $p < 0.001$

order to further confirm the role of PRT4165 in primary cells model, we constructed a primary $CD4^+$T lymphocyte latent model again, and similar results were obtained with cell lines (Fig. 6D).

Considering that PRT4165 mainly acts as an epigenetic inhibitor, it may play an enhancing role rather than a switching role in the process of gene transcription. Therefore, we speculate that PRT4165 may have a good synergistic activation effect with the reported latent activators. Therefore, we selected different latent activators, including histone deacetylase inhibitor SAHA (0.50 μM), BET inhibitor JQ1 (0.01 μM), and PKC agonist (0.01 μM), DNA methylation inhibitors 5-aza (1 μM), to try to synergize with PRT4165 (10 μM). We found that PRT4165 with JQ1, SAHA and 5-aza have good synergistic activation effects, but not so well with PEP005 (Fig. 6E). Then, we constructed a primary $CD4^+$ T lymphocyte latent model again, and confirmed that PRT4165 alone had a slight activation effect on the primary latent model, but combined PEP005, it has a good synergistic activation effect (Fig. 6F), which further confirms that PRT4165 can be used as a good synergistic activator drug.

PRT4165 displays minimal toxicity in primary $CD4^+$T cells

Currently, latent activators agents suitable for clinical studies should have low toxicity characteristics. To evaluate the cytotoxicity of PRT4165, we first detected the cell proliferation activity through CCK8 in C11 cells, J-Lat10.6 cells, ACH2 cell and PBMC. The results showed that PRT4165 (10 μM) had little effect on the proliferation activity of PBMCs (Supplemental Fig. S6A–S6D). In addition, we found that PRT4165 does not significantly cause cell apoptosis (Supplemental Fig. S6E–S6 H). Besides, we further evaluated the impact of PRT4165 on the immune activation status of PBMCs. The results indicated that there was no significant difference in the expression levels of CD25 and CD69 in PBMCs, suggesting that PRT4165 does not have an immune-activating effect on PBMCs at its working concentration (10 μm) (Supplemental Fig. S7).

Discussion

In this study, we conducted an enChIP to identify the proteins potentially interacting with the HIV-1 L region with FLAG-ZFP in a HIV latently infected cell line model. Our data identified a series of transcription factors that have been previously reported to bind to the HIV-1 L region, including HDAC2, HMGB1, SP-1, NF-kB, etc. More importantly, we also identified many proteins that have not been previously reported to be related to HIV-1 latency. Among them, we found that RYBP can act as an adapter protein, cooperating with the YY1 protein bound to the HIV-1 L region, recruiting KDM2B. RYBP and KDM2B together changed the methylation and ubiquitination modification levels of the protein near the HIV-1 L, and promoted HIV-1 latency. These results suggested that RYBP may be a potential new HIV-1 latent activation target.

Based on our cumulative data, we proposed a working model that RYBP restricts HIV-1 transcription and is associated with HIV-1 latency (Fig. 7). In the latent state, RYBP is recruited by YY1 to the HIV-1 L region, affecting the level of histone H2AK119ub. Besides, RYBP also recruits KDM2B to affect the level of H3K4me3, inhibiting HIV-1 transcriptional elongation by changing epigenetic genetic modifications, thereby promoting HIV-1 latency. When the virus is activated, the viral protein Tat will inhibit the expression of RYBP, thereby destroying the inhibitory effect of RYBP on HIV-1, promoting viral transcription and replication.

Prior to this study, researchers had found that there is a correlation between histone H2AK119ub levels and HIV-1 latency, but how this process is regulated is unknown [37]. In addition, Ma et al. also discovered the molecular mechanism by which PRC1 classical complex subunit CBX4 regulates EZH2 activity in a liquid-phase separation form to promote HIV-1 latent infection [38]. However, whether the non-classical form of the PRC1, namely RYBP, is involved in HIV-1 latency and its mechanism of action have not been reported before this study. Therefore, our study suggested that the PRC1 may be a potential HIV-1 latency activation target. At the same time, we also found that the PRC1 inhibitor PRT4165 can activate latent HIV-1, and PRT4165 has good synergy with the above LRA.

However, our study currently has some limitations. First, during the viral transcription and replication stage, Tat protein downregulates the expression of RYBP. It is also an interesting question how the Tat protein facilitates viral immune evasion and what mechanisms are involved. Second, the activation of latent HIV-1 by PRT4165 is currently limited to the cellular level, and further studies are required to assess its efficacy in animal models and in patients.

Conclusion

In summary, in this study, through enChIP technology based on FLAG-ZFP protein, we newly identified a protein-RYBP that can interact with the HIV-1 L region and change the epigenetic modification of histones near the LTR region, thus promoting HIV-1 Latency. Besides, inhibition of RYBP, whether at the genetic level or pharmacologically, can promote HIV-1 latent activation. Our study not only deepens our understanding of the molecular mechanism of HIV-1 latency, but also shows that RYBP is a new potential HIV-1 latency activation target.

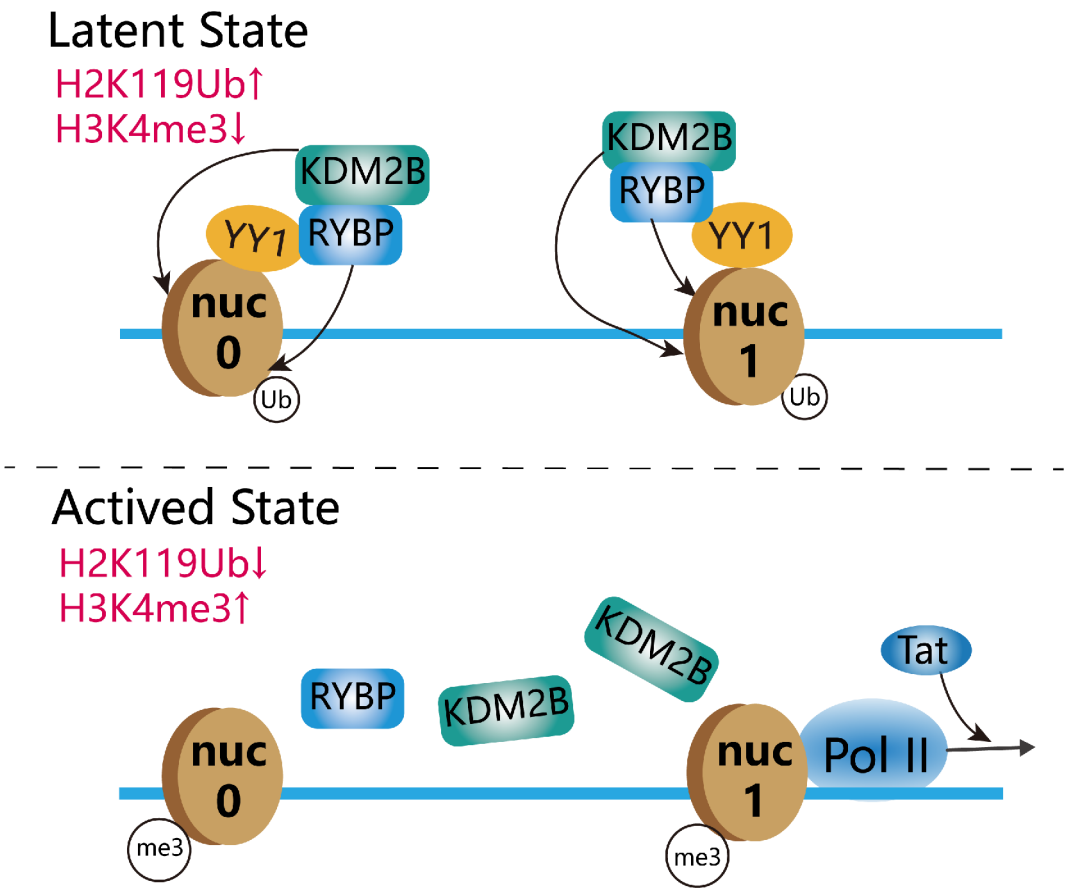

Fig. 7 A working model of the role of RYBP and KDM2B in the establishment of HIV latency

Abbreviations

HIV-1	Human immunodeficiency virus-1
AIDS	Acquired immunodeficiency syndrome
enChIP	engineered chromatin immunoprecipitation
ZFP	Zinc finger nucleic acid proteins
ChIP	Chromatin immunoprecipitation
YY1	Yin Yang 1
LTR	Long terminal repeats
ART	Antiretroviral therapy
PRC1	Polycomb-repressive complex 1
GFP	Green fluorescent protein
PBS	Phosphate buffered saline
ELISA	Enzyme-Linked Immunosorbent Assay
PCR	Polymerase chain reaction

Supplementary Information

The online version contains supplementary material available at https://doi.org/10.1186/s12964-025-02221-z.

Supplementary Material 1

Supplementary Material 2

Supplementary Material 3

Author contributions

HZ.Z. and XY.Y. conceived and designed the experiments. HZ.L., YZ.S. and J.C. provided key clinical patient samples. XY.Y., YQ.Z. and XY.Z. carried out most experiments. JN.X. completed the testing and follow-up of clinical samples. XY.W., YP.C., CY.L., XY.Y., DQ.W. and ZL.H. participated in some of the experiments. HZ.Z.,XY.Y., YQ.Z., XY.Z. and SB.J. directed and supervised the experiments and interpretation of data. XY.Y. and HZ.Z. wrote the paper. All authors have read and approved the manuscript being submitted.

Funding

This study was funded by the National Natural Science Foundation of China (82402609 to XYY) and the National Key Research and Development Program of China (2023YFC2306700 to HZZ, 2024YFC2300110 to XYY). All funding parties did not have any role in the design of the study or in the explanation of the data.

Data availability

All data are available upon request, and queries shoud be sent to hzzhu@fudan.edu.cn and xinyy@fudan.edu.cn.

Declarations

Competing interests

The authors declare no competing interests.

Author details

[1]State Key Laboratory of Genetic Engineering and Engineering Research Center of Gene Technology, Ministry of Education, Institute of Genetics, School of Life Sciences, Yiwu Research Institute of Fudan University, Fudan University, Shanghai, China
[2]Yunnan Provincial Infectious Diseases Hospital/Yunnan AIDS Care Center, Kunming, China
[3]Scientific Research Center, Shanghai Public Health Clinical Center, Fudan University, Shanghai, China
[4]Department of Infectious Disease, The Second Hospital of Nanjing, Nanjing University of Chinese Medicine, Nanjing Medical University, Center for Global Health, School of Public Health, Nanjing, China

[5]Department of Infectious Diseases and Immunology, Shanghai Public Health Clinical Center, Fudan University, Shanghai, China
[6]Department of Infectious Diseases and Nursing Research Institution, National Clinical Research Center for Infectious Diseases, The Third People's Hospital of Shenzhen, Shenzhen, Guangdong, China
[7]Key Laboratory of Medical Molecular Virology (MOE/NHC/CAMS), Shanghai Institute of Infectious Disease and Biosecurity, School of Basic Medical Sciences, Fudan University, Shanghai, China

Received: 7 January 2025 / Accepted: 28 April 2025
Published online: 13 May 2025

References

1. Bailey H, Zash R, Rasi V, Thorne C. HIV treatment in pregnancy. Lancet HIV. 2018;5(8):e457–67.
2. Kanters S, Vitoria M, Doherty M, Socias ME, Ford N, Forrest JI, et al. Comparative efficacy and safety of first-line antiretroviral therapy for the treatment of HIV infection: a systematic review and network meta-analysis. Lancet HIV. 2016;3(11):e510–20.
3. Margolis DM, Archin NM, Cohen MS, Eron JJ, Ferrari G, Garcia JV, et al. Curing HIV: seeking to target and clear persistent infection. Cell. 2020;181(1):189–206.
4. Chun TW, Engel D, Berrey MM, Shea T, Corey L, Fauci AS. Early establishment of a pool of latently infected, resting CD4(+) T cells during primary HIV-1 infection. Proc Natl Acad Sci U S A. 1998;95(15):8869–73.
5. Finzi D, Hermankova M, Pierson T, Carruth LM, Buck C, Chaisson RE, et al. Identification of a reservoir for HIV-1 in patients on highly active antiretroviral therapy. Science. 1997;278(5341):1295–300.
6. D'Orso I. HIV-1 transcription and latency in the spotlight. Viruses. 2024;16(2):248.
7. Moar P, Premeaux TA, Atkins A, Ndhlovu LC. The latent HIV reservoir: current advances in genetic sequencing approaches. mBio. 2023;14(5):e0134423.
8. Kim Y, Anderson JL, Lewin SR. Getting the kill into shock and kill: strategies to eliminate latent HIV. Cell Host Microbe. 2018;23(1):14–26.
9. Lusic M, Giacca M. Regulation of HIV-1 latency by chromatin structure and nuclear architecture. J Mol Biol. 2015;427(3):688–94.
10. Verdin E, Paras P Jr, Van Lint C. Chromatin disruption in the promoter of human immunodeficiency virus type 1 during transcriptional activation. EMBO J. 1993;12(8):3249–59.
11. Jordan A, Bisgrove D, Verdin E. HIV reproducibly establishes a latent infection after acute infection of T cells in vitro. EMBO J. 2003;22(8):1868–77.
12. Einkauf KB, Osborn MR, Gao C, Sun W, Sun X, Lian X, et al. Parallel analysis of transcription, integration, and sequence of single HIV-1 proviruses. Cell. 2022;185(2):266–e28215.
13. Einkauf KB, Osborn MR, Gao C, Sun W, Sun X, Lian X, et al. A Two-Color haploid genetic screen identifies novel host factors involved in HIV-1 latency. mBio. 2021;12(6):e0298021.
14. Boehm D, Jeng M, Camus G, Gramatica A, Schwarzer R, Johnson JR, et al. SMYD2-Mediated histone methylation contributes to HIV-1 latency. Cell Host Microbe. 2017;21(5):569–e5796.
15. Huang H, Kong W, Jean M, Fiches G, Zhou D, Hayashi T, et al. A CRISPR/Cas9 screen identifies the histone demethylase MINA53 as a novel HIV-1 latency-promoting gene (LPG). Nucleic Acids Res. 2019;47(14):7333–47.
16. Jiang G, Nguyen D, Archin NM, Yukl SA, Méndez-Lagares G, Tang Y, et al. HIV latency is reversed by ACSS2-driven histone crotonylation. J Clin Invest. 2018;128(3):1190–8.
17. Lusic M, Marcello A, Cereseto A, Giacca M. Regulation of HIV-1 gene expression by histone acetylation and factor recruitment at the LTR promoter. EMBO J. 2003;22(24):6550–61.
18. Wightman F, Ellenberg P, Churchill M, Lewin SR. HDAC inhibitors in HIV. Immunol Cell Biol. 2012;90(1):47–54.
19. Li JH, Ma J, Kang W, Wang CF, Bai F, Zhao K, et al. The histone deacetylase inhibitor Chidamide induces intermittent viraemia in HIV-infected patients on suppressive antiretroviral therapy. HIV Med. 2020;21(11):747–57.
20. Imai K, Togami H, Okamoto T. Involvement of histone H3 lysine 9 (H3K9) methyltransferase G9a in the maintenance of HIV-1 latency and its reactivation by BIX01294. J Biol Chem. 2010;285(22):16538–45.
21. Ding D, Qu X, Li L, Zhou X, Liu S, Lin S, et al. Involvement of histone methyltransferase GLP in HIV-1 latency through catalysis of H3K9 dimethylation. Virology. 2013;440(2):182–9.
22. Friedman J, Cho WK, Chu CK, Keedy KS, Archin NM, Margolis DM, et al. Epigenetic Silencing of HIV-1 by the histone H3 lysine 27 methyltransferase enhancer of Zeste 2. J Virol. 2011;85(17):9078–89.
23. Yang X, Zhao X, Zhu Y, Shen Y, Wang Y, Lu P, et al. FKBP3 induces human immunodeficiency virus type 1 latency by recruiting histone deacetylase 1/2 to the viral long terminal repeat. mBio. 2021;12(4):e0079521.
24. Yang X, Zhao X, Zhu Y, Xun J, Wen Q, Pan H, et al. FBXO34 promotes latent HIV-1 activation by post-transcriptional modulation. Emerg Microbes Infect. 2022;11(1):2785–99.
25. Laird GM, Bullen CK, Rosenbloom DI, Martin AR, Hill AL, Durand CM, et al. Ex vivo analysis identifies effective HIV-1 latency-reversing drug combinations. J Clin Invest. 2015;125(5):1901–12.
26. Wang P, Qu X, Wang X, Zhu X, Zeng H, Chen H, et al. Specific reactivation of latent HIV-1 with designer zinc-finger transcription factors targeting the HIV-1 5'-LTR promoter. Gene Ther. 2014;21(5):490–5.
27. Barton KM, Archin NM, Keedy KS, Espeseth AS, Zhang YL, Gale J, et al. Selective HDAC Inhibition for the disruption of latent HIV-1 infection. PLoS ONE. 2014;9(8):e102684.
28. Gougeon ML, Melki MT, Saïdi H. HMGB1, an alarmin promoting HIV dissemination and latency in dendritic cells. Cell Death Differ. 2012;19(1):96–106.
29. Ran XH, Zhu JW, Ni RZ, Zheng YT, Chen YY, Zheng WH, et al. TRIM5α recruits HDAC1 to p50 and Sp1 and promotes H3K9 deacetylation at the HIV-1 LTR. Nat Commun. 2023;14(1):3343.
30. Yang X, Wang Y, Lu P, Shen Y, Zhao X, Zhu Y, et al. PEBP1 suppresses HIV transcription and induces latency by inactivating MAPK/NF-κB signaling. EMBO Rep. 2020;21(11):e49305.
31. Verdikt R, Hernalsteens O, Van Lint C. Epigenetic mechanisms of HIV-1 persistence. Vaccines (Basel). 2021;9(5):514.
32. Coull JJ, Romerio F, Sun JM, Volker JL, Galvin KM, Davie JR, et al. The human factors YY1 and LSF repress the human immunodeficiency virus type 1 long terminal repeat via recruitment of histone deacetylase 1. J Virol. 2000;74(15):6790–9.
33. Isshiki Y, Nakajima-Takagi Y, Oshima M, Aoyama K, Rizk M, Kurosawa S, et al. KDM2B in polycomb repressive complex 1.1 functions as a tumor suppressor in the initiation of T-cell leukemogenesis. Blood Adv. 2019;3(17):2537–49.
34. Ciapponi M, Karlukova E, Schkölziger S, Benda C, Müller J. Structural basis of the histone ubiquitination read-write mechanism of RYBP-PRC1. Nat Struct Mol Biol. 2024;31(7):1023–7.
35. Horvath RM, Sadowski I. CBP/p300 lysine acetyltransferases inhibit HIV-1 expression in latently infected T cells. iScience. 2024;27(12):111244.
36. Zhang CZ, Chen SL, Wang CH, He YF, Yang X, Xie D, et al. CBX8 exhibits oncogenic activity via AKT/β-Catenin activation in hepatocellular carcinoma. Cancer Res. 2018;78(1):51–63.
37. Yoon CH, Jang DH, Kim KC, Park SY, Kim HY, Kim SS, et al. Disruption of polycomb repressor complex-mediated gene Silencing reactivates HIV-1 provirus in latently infected cells. Intervirology. 2014;57(2):116–20.
38. Wu L, Pan T, Zhou M, Chen T, Wu S, Lv X, et al. CBX4 contributes to HIV-1 latency by forming phase-separated nuclear bodies and sumoylating EZH2. EMBO Rep. 2022;23(7):e53855.

Publisher's note